Journal of the European Ceramic Society **13** (1994) 11–23

Deformation of Ceria-Stabilised Tetragonal Zirconia Ceramics in Scratch Experiments with a Sharp Indenter

Anoop K. Mukhopadhyay,* Tianshun Liu, Michael V. Swain & Yiu-Wing Mai

Center for Advanced Materials Technology, Department of Mechanical Engineering, University of Sydney, New South Wales 2006, Australia

(Received 29 January 1993; revised version received 30 July 1993; accepted 13 September 1993)

Abstract

With a view to understanding the friction and deformation behaviour of tough zirconia polycrystals under conditions of severe contact stress, single pass scratch experiments were conducted with a Vickers indenter on ceria-stabilised tetragonal zirconia ceramics having grain sizes varying from 0·5 to 2·7 μm. For a given grain size, the frictional force, the width, depth and hence the volume of wear groove as well as the transformation zone size (h) all increased with applied normal load (8–20 N). At a given load, the transformation zone size increased with grain size. The deformation behaviour was characterised predominantly by plastic ploughing and to a small extent by other components such as localised microcracking, grain boundary microfracture and chipping. A brief comparison of these results with previous work on alumina, a typical non-phase-transforming ceramic, is also presented, with a view to highlight the distinction in deformation and wear behaviour of the two different type of ceramics.

Das Reibungs- und Verschleißverhalten von mit Zeriumoxid stabilisiertem, tetragonalem polykristallinem Zirkoniumoxid mit einer Korngröße von 0·5–2·7 μm wurden mit Hilfe eines Vickers Eindruckstempels in einem Ritztest untersucht. Bei gegebener Korngröße nimmt die Reibungskraft, die Beite, Tiefe und das Volumen der Rille sowie die Größe (h) der Transformationszone mit der aufgebrachten Last (8–20 N) zu. Bei gegebener Last nimmt h mit der Korngröße zu. Die Prozesse, die zur Verschleißschädigung führen, werden hauptsächlich durch plastisches Furchen und zu einem geringeren Teil durch die lokale Bildung von Mikrorissen, Korngrenzenmikrobruch und Ausbrechen verursacht.

Afin de mieux comprendre le comportement en friction et en déformation des polycristaux de zircone tétragonale soumis a d'importantes contraintes de contact, nous avons mené des expériences de rayure par un seul passage avec un indenteur Vickers sur des céramiques de zircone tétragonale cériée dont la taille de grains varie de 0·5 à 2·7 μm. Pour une taille de grains donnée, la force de frottement, la largeur, la profondeur et donc le volume du sillon d'usure, de même que la taille de la zone de transformation (h) augmentent tous avec la force normale appliquée (8N–20N). Pour une force donnée, la taille de la zone de transformation augmente avec la taille des grains. La caractéristique principale du comportement en déformation est la formation d'un rebord le long du sillon et, dans une moindre mesure, de la microfissuration localisée, du taillage par éclats et de la fracture microscopique aux joints de grains. Une brève comparaison de ces résultats avec notre étude précédente sur l'alumine, cas typique de céramique sans transformation de phase, est également présentée pour montrer les différences de comportement en déformation et à l'usure de ces deux types de céramiques.

1 Introduction

Zirconia (ZrO_2) based ceramics have strength, hardness and fracture toughness considered as exceptionally high in comparison to their brittle counterparts. The combination of these properties has enhanced the candidature of zirconia ceramics for wear resistant applications.[1–4] In fact, enhanced toughness values of about 10–20 MPa $m^{1/2}$ are reported to be realisable through proper control of microstructure and phase transformation.[1] The crack shielding induced by the phase transformation is thought to be the main contributor to enhanced toughness.[1] In spite of the exceptional toughness

* Present address: Electroceramics Division, Central Glass & Ceramic Research Institute, Calcutta 700032, India.

properties of the Ce-TZP ceramics (ceria-stabilised tetragonal zirconia polycrystals) related to their transformation plasticity,[5] most of the reported work concentrate on friction and wear behaviour of PSZ (partially stabilised zirconia) and Y-TZP (yttria-stabilised tetragonal zirconia) ceramics.[2,4,6] Friction and wear behaviour of zirconia ceramics are found to be a sensitive function of the microstructural parameters such as porosity and grain size, contact stress, the extent and intensity of stress-induced tetragonal (t) to monoclinic (m) phase transformation, atmosphere and temperature. Several features observed on the worn surfaces include plastic deformation, delamination and grain fracture.[2,4,6,7] However, because the worn surface contains too much damage, these investigations fail to identify the wear mechanisms clearly.

In this connection, single pass scratch experiments offer potential alternative in the sense that they can elucidate the mechanism of wear initiation in perspective of abrasive wear. Only limited scratch experiments are reported for Y-TZP[2] at loads of 100–200 N, while for other ceramics such as alumina the range of load investigated is from 0·1 to 1 N.[3] The role of mechanical properties in the control of wear behaviour is not very clear in the case of ZrO_2-based ceramics, particularly when environmentally assisted crack growth is promoted.[8,9] Insofar as Ce-TZP is concerned, only a couple of investigations are available.[10,11] Transmission electron microscopic observations in the sub-surface regions of Vickers indentations made at 300 N load on a 12 mol% Ce-TZP provided evidence for the absence of any dislocation generation.[11] This has the implication that all the plasticity and the necessary ductility were manifested by the stress-induced t→m transformation that occurred around the indents. In the manually ground and diamond ground surfaces of the same material, on the other hand, significant differences were found between the monoclinic phase contents.[10] Only limited amounts of monoclinic phase could be detected on the diamond ground surface, whereas the same was present to a significantly higher extent on the manually ground surface. These apparently contradictory results have been explained in terms of stress-induced t→m transformation.

The purpose of the present work was to identify the influence of grain size vis-à-vis phase transformation on the friction and wear characteristics in single pass scratch tests at a constant speed of 6 mm/s and under moderate normal loads of about 8 N to 20 N on 9 mol% Ce-TZP ceramics fabricated in a controlled manner[12] to have grain sizes spanning the range 0·5 μm to 2·7 μm. In addition, just for the purpose of comparison, data from the authors' earlier work on wear of a typical non-phase-transforming ceramic, e.g. alumina, has been included to illustrate the distinction of its deformation and contact damage characteristics from the present phase-transforming ceramics.

2 Experimental Methods

Details of the material synthesis and microstructural characterisation have been published elsewhere.[12] Briefly, the CeO_2–ZrO_2 powder containing 9 mol% CeO_2 and trace impurities (HfO_2, SiO_2) was obtained from a commercial supplier (Ce-14, Unitec Ceramics Ltd, Stafford, UK) and conventionally sintered. Density measurements by the water immersion technique gave values between 97·6% and 99·8% of the theoretical value. Grain size measurements by the linear intercept technique gave average values of 0·5 μm, 1·0 μm, 1·4 μm, 1·5 μm and 2·7 μm for the Ce-TZP1, Ce-TZP2, Ce-TZP3, Ce-TZP4 and Ce-TZP5 materials, respectively. The monoclinic phase contents in the different Ce-TZP materials were measured on ground as well as fractured surfaces using X-ray diffractometry. Typical average scatter of the phase contents was less than 5% and 8% for the ground and fractured surfaces, respectively. The alumina ceramics used for wear tests were prepared from high purity alumina powders of submicron particle size.[13] Specimens of grain sizes 0·7 μm, 5·0 μm and 25·0 μm were used for the wear tests.

Detailed descriptions of the preparation of alumina samples as well as the experimental methods used for the scratch tests have been reported elsewhere.[13] In short, the scratch experiments were conducted in a reciprocating sliding machine built in the authors' own laboratory. A sharp Vickers indenter of apex angle 136° and tip radius less than 0·5 μm was used on polished and annealed (500°C, 30 min in air) rectangular specimens measuring $10 \times 6 \times 4\,mm^3$. The tangential force of friction (F) was measured using a LVDT and the scratching speed was 6 mm/s. The deadweight of the loading assembly produced an effective force of 8 N at the indenter and in the scratch experiments the normal load was varied between 8 N and 20 N using an adjustable lever arm. In the single pass tests the loaded indenter scratched the sample surface once with a leading plane. Care was taken in assuming the vertical alignment of the indenter on the sample surface by visual inspection. After each single test the indenter was cleaned with ethanol to remove any adhered wear debris. In the case of the alumina samples identical test conditions were used with a blunt diamond indenter of about 100 μm tip radius[13,14] in addition to the same sharp indenter. Average values of the groove width and depth were

obtained from at least two experiments using scanning electron microscopy (SEM) and surface profilometry techniques using a high resolution profilometer (Talysurf, Hobson, UK, resolution better than 5 nm). Several cross-sectional measurements were made at various positions along the length of the scratch to have a reliable estimate of the groove depth. The error bars included in the experimental results presentation signify typical average scatter in data. The force ratio (f) was calculated as the ratio of tangential (F) to normal (P) forces. The wear volume was calculated from the measured values of groove width and depth assuming a triangular cross-section using the length of the

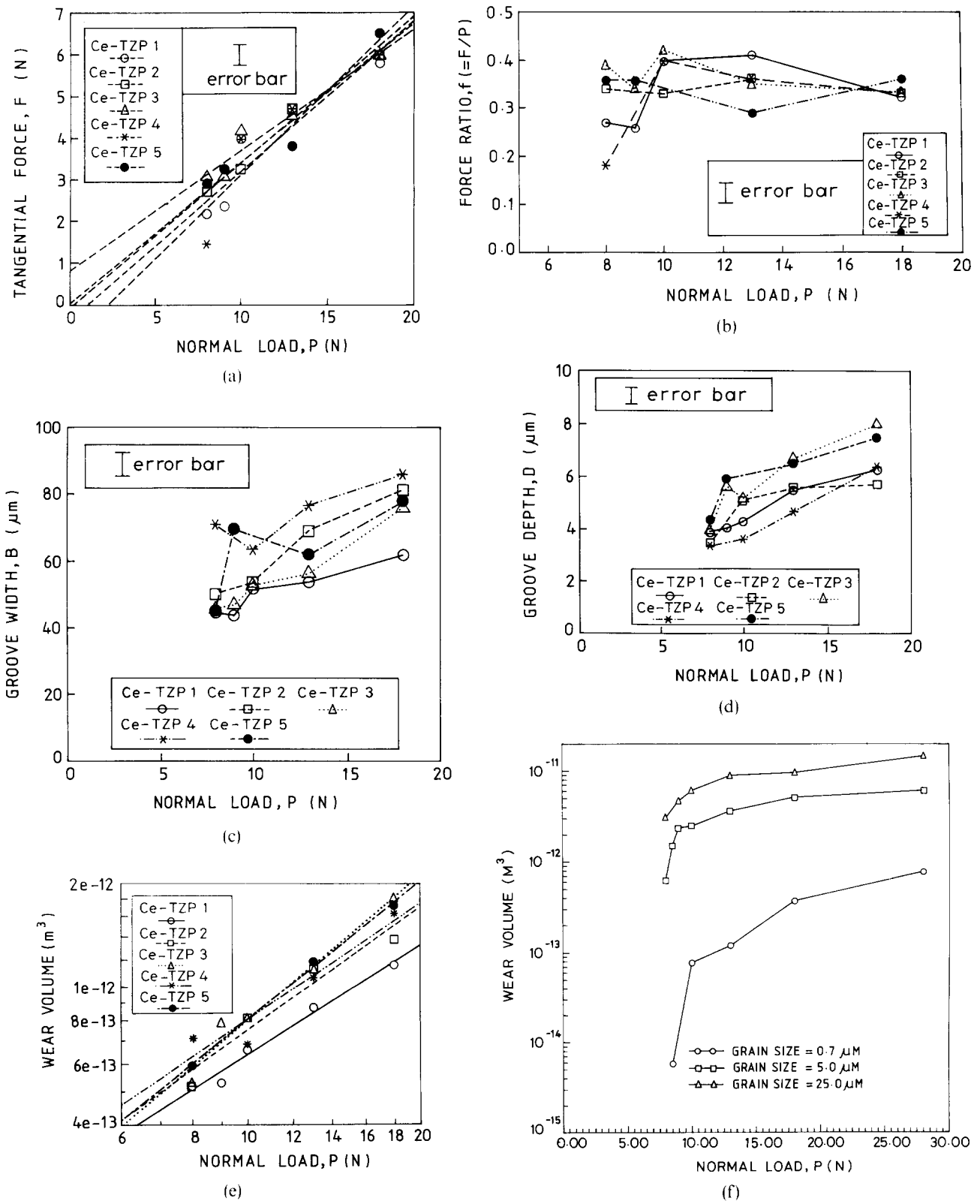

Fig. 1. Variation of (a) tangential force (F) and (b) force ratio (f) with normal load (P) for Ce-TZP. Relationship between (c) groove width (B) and (d) groove depth (D) and normal load (P) for Ce-TZP. Effect of normal load (P) on wear volume of (e) Ce-TZP and (f) alumina ceramics (from Ref. 14).

groove (6 mm) as the other dimension. The wear damage process was studied with the aid of optical as well as SEM techniques.

3 Experimental Results

3.1 Scratch characteristics

Figures 1(a)–(e) show the effects of increasing the normal load on the scratch characteristics in the single pass tests. For a given grain size of Ce-TZP, the tangential force (F), the width (B), the depth (D) and hence the wear volume all increased with normal load (P). The force ratio (f), however, seemed to be insensitive to variation in applied normal load as well as grain sizes; see Fig. 1(b). The wear volume generally exhibits a power law dependence on the normal load; see Fig. 1(e). These results compare favourably with those reported for Y-TZP, PSZ, alumina and various other ceramics.[2,3,5,7,13–15] However, comparisons of the present results with the present authors' previous work[13,14] on alumina ceramics, Fig. 1(f), indicates that a strong grain size effect in abrasive wear exists in the case of alumina, while the wear volume of the present Ce-TZP ceramics seem to be insensitive to variation in grain size (compare Figs 1(e) and (f)). Although the data shown in Fig. 1(f) was for abrasive contact with a blunt diamond indenter,[14] an exactly similar trend was noted in experiments[13] conducted with the same sharp Vickers indenter as was used for the present Ce-TZP ceramics. In other words, depending on the indenter shape, the relative magnitude of calculated values of the wear volume changes but the strong influence of grain size on wear volume was always exhibited by the alumina ceramics.[13,14]

Figure 2 shows the effect of increasing the normal load on the transformation zone size (h) as a function of the grain size. As before, the error bars signify typical average scatter in the zone size data. For a given grain size, the transformation zone size surrounding the scratch always increased with increasing applied normal load. At a given load, the transformation zone size showed an increasing trend with respect to grain size. For the purpose of comparison the monoclinic phase contents

$$(m)/(m + t + c)\%$$

on the ground surface as well as on the fracture surface of the five Ce-TZP materials are plotted in the same figure as a function of the grain size. On the ground surface the monoclinic phase content increased with grain size. The trend was similar for the fractured surface, except that the relative magnitude of the monoclinic phase was higher. Also, particularly for grain sizes above 1 μm, the relative

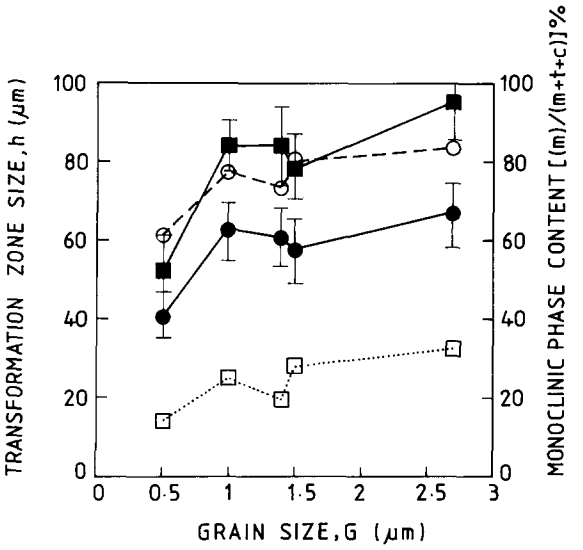

Fig. 2. Relationship between the transformation zone size (h), grain size (G) and monoclinic phase content [(m)/(m + t + c)]%, on the scratched (●, $P = 8$ N; ■, $P = 18$ N), ground (□) and fractured (○) surfaces of Ce-TZP.

scatter in phase content estimation was slightly on the higher side for both ground as well as fractured surfaces. Although an exact estimation of the monoclinic phase content on the scratched surface could not be done, it seems reasonable to assume on the basis of experimental data on ground and fracture surfaces that the monoclinic phase content on the scratched surface may be somewhere between the cases of fractured and ground surfaces. As a typical example, Figs 3(a) and (b) show the Nomarski interference optical micrographs of scratches produced under normal loads of 8 N and 18 N respectively, in the Ce-TZP1 material of grain size 0·5 μm. Notice that the width of transformation zone beside the scratch is indeed very small. It appears that there is a small surface uplift in these regions. In contrast, the Ce-TZP5 material with the coarsest grain size of 2·7 μm shows an appreciable transformation zone at both 8 N and 18 N normal loads, Figs 3(c) and (d), during the single pass scratch experiments. Here the surface uplift is more obvious. Such surface uplift has been observed also during static indentation studies using a Vickers indenter and has been related to the transformation plasticity.[6,11]

3.2 Damage processes

The microstructure of brittle materials, particularly those exhibiting rising crack growth resistance characteristics with respect to crack extension, can exhibit significant influence on their wear behaviour.[16] Figures 4(a) to (e) show the microstructures of the five Ce-TZP materials as revealed on the fractured surfaces of room-temperature inert strength tests samples.[12] The extent of intergranular fracture was more in the coarse-grained materials than in the fine-grained material Ce-TZP1.

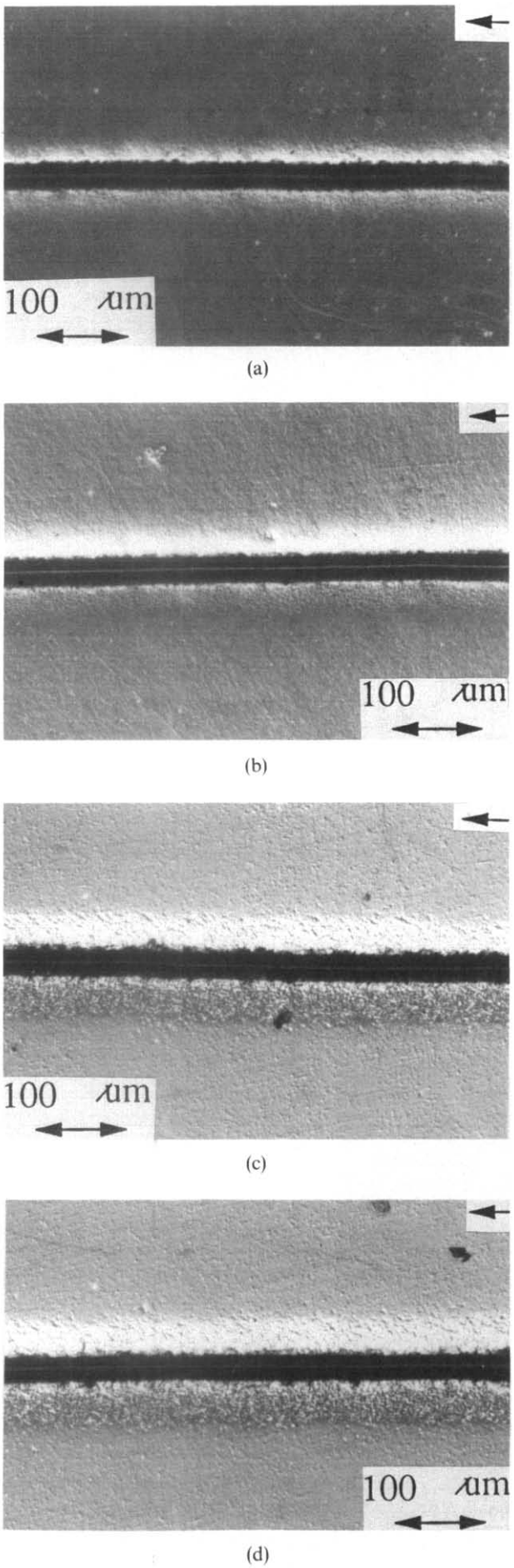

Fig. 3. Transformation zone around scratch made at (a) $P = 8$ N and (b) $P = 18$ N on 0·5 μm grain size Ce-TZP, and (c) $P = 8$ N and (d) $P = 18$ N on 2·7 μm grain size Ce-TZP.

Typical examples of scratches made at relatively low loads of 8 N or 10 N are shown in Fig. 5(a) and (b) for the Ce-TZP1 and Ce-TZP3 ceramics, respectively. In these and the subsequent photomicrographs the arrows indicate the sliding direction of the indenter. Ce-TZP1 and Ce-TZP3 had grain sizes of 0·5 μm and 1·4 μm, respectively. The main mode of deformation for these materials appears to be plastic ploughing. Also, there is no significant difference between the deformation modes of very fine-grain sized material and the relatively coarse-grain sized material. The micrograph of Fig. 5(b) was taken from near the beginning of scratch generated by the leading plane of the indenter. However, the appearance of some crack-like features near the sides of the groove indicates that probably a considerable amount of friction has occurred in those regions. This has the implication that the applied normal load was carried not only by the leading plane but also by the two planes adjacent to the leading plane of the indenter. Figures 5(c) and (d) illustrate the high magnification views of the crack-containing regions already discussed.

Both in the fine-grained Ce-TZP1 and in the relatively coarse-grained Ce-TZP3 these features are very nearly similar. The cracks appear at an angle to the scratching direction and are nearly parallel to each other. In Ce-TZP1 the mode of crack propagation seems to be intergranular. Also there is a slight tendency of sub-surface fracture propagation in the region very close to the groove; see Fig. 5(c). In the case of Ce-TZP3, however, a heavily deformed layer appears to be present throughout the cross-section of the groove; see Fig. 5(d).

Increasing the load usually resulted in small amount of additional grain boundary microfracture near the edge of the plastically deformed groove; see Fig. 6(a). At the highest applied load of 18 N, typically the groove was characterised by a heavily deformed region near the middle of the groove and a slightly damaged region near the edge of the groove; see Fig. 6(b). In the case of the 1·0 μm grain size Ce-TZP material, there appears to be a small amount of very local chipping which has caused removal of thin layers of material in isolated areas. The presence of microcracks in the groove is also very noticeable. At high magnification, Fig. 6(c), these microcracks seem to be interconnected in a few regions and the entire region where these cracks form appears heavily deformed.

In the case of alumina ceramics, on the other hand,[14] at loads less than 10 N the wear damage was mainly plastic deformation-controlled in the 0·7 μm grain sized material. At loads above 10 N the wear damage exhibited a mixed control of plastic deformation and brittle fracture. For grain sizes higher than 0·7 μm the wear damage was always

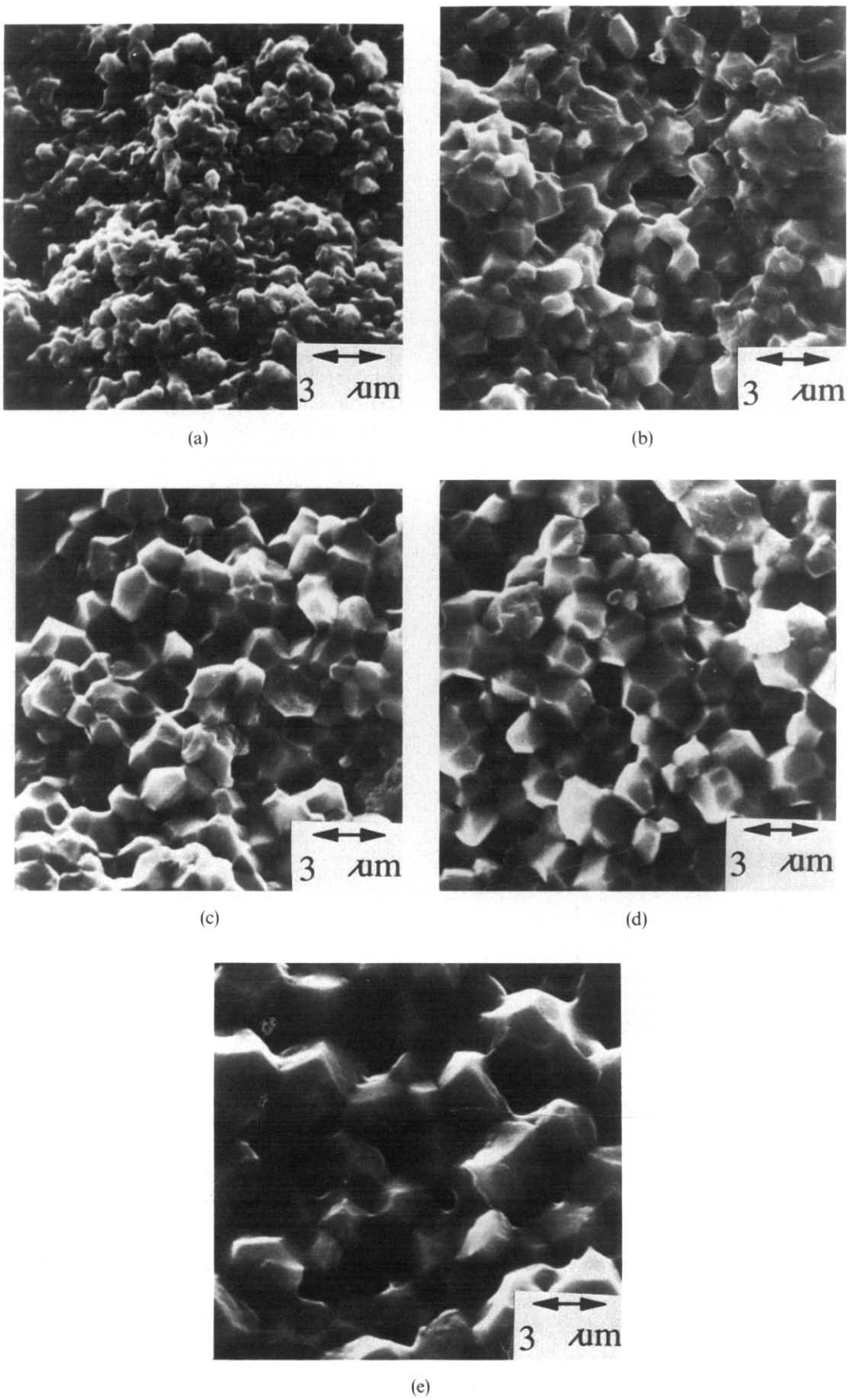

Fig. 4. Microstructures of (a) 0·5 μm, (b) 1·0 μm, (c) 1·4 μm, (d) 1·5 μm and (e) 2·7 μm grain size Ce-TZP.

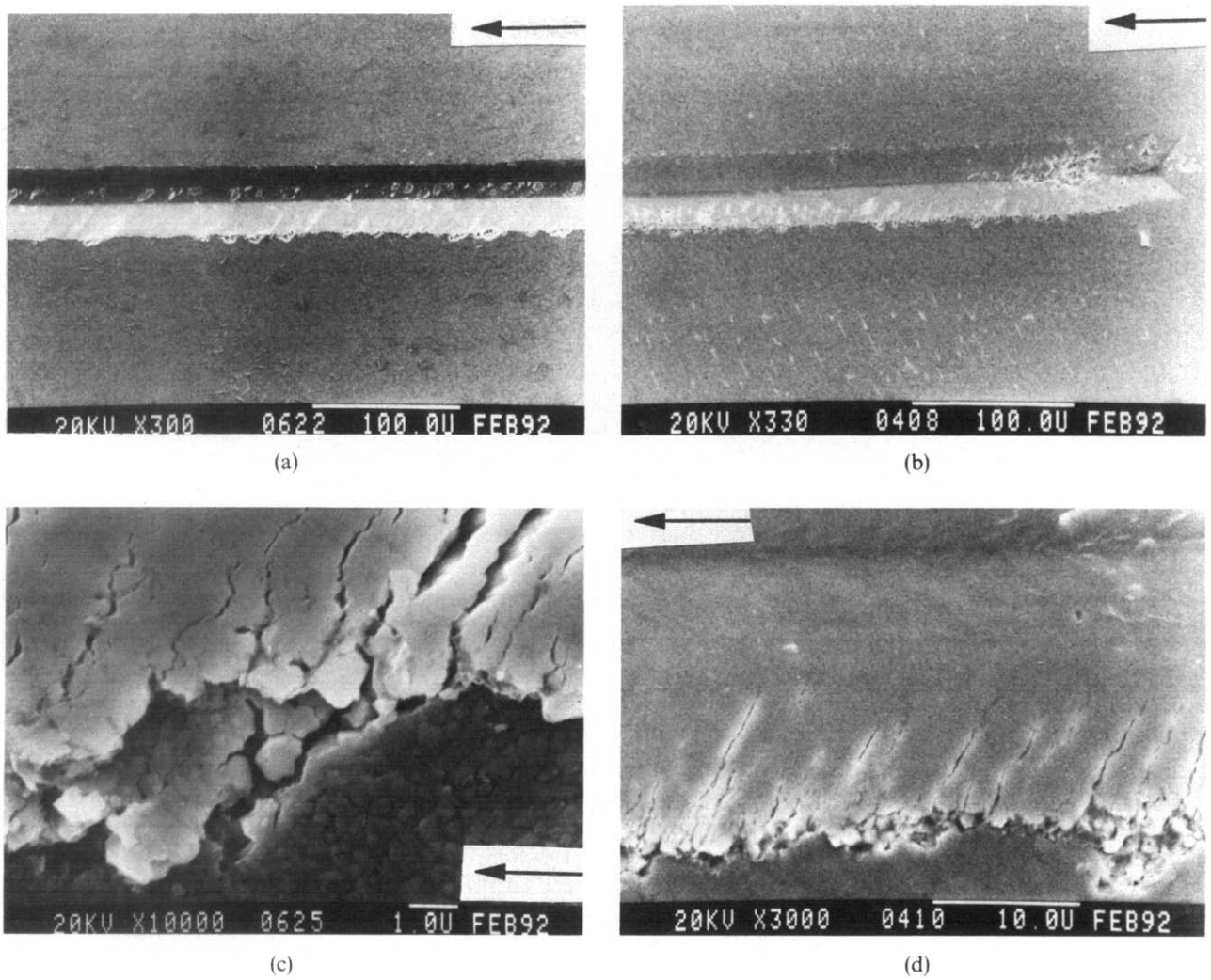

Fig. 5. Scratch made at (a) $P = 10$ N on 0·5 μm and (b) $P = 8$ N on 1·4 μm grain size Ce-TZP. High magnification view of microcrack-rich region (c) in Fig. 5(a) and (d) in Fig. 5(b).

brittle fracture-controlled, corresponding to the normal load range of 8–40 N. Thus, the wear damage processes in the present transforming and non-transforming ceramics are different.

4 Discussion

4.1 Deformation characteristics

In the single pass scratch experiments the tangential force of friction varies linearly with the normal load on the pyramidal indenter. Similar behaviour has been reported from low-load and high-load scratch experiments at low speed on hot pressed and sintered alumina.[3,14] The ratio of tangential to normal forces, f, however, does not vary appreciably with load; see Fig. 1(b). The present force ratio values span a range from about 0·2 to 0·4. These values are comparable to the friction coefficient data for PSZ[5] and Y-TZP,[7,9] although the experimental conditions are very different.

According to the ploughing theory of friction,[17] the load independence of force ratio is expected. To illustrate this point it is noted that the scratches were made with one leading plane. However, as discussed in Section 3.2 and the micrographs presented therein, see e.g. Fig. 5(b), most probably the two planes adjacent to the leading plane were also in contact and bore the load. Under such a situation, the force ratio, f, is given by[17]

$$f = [\{\mathrm{Cot}\,\theta + \mu(1 + 2\,\mathrm{Cosec}\,\theta)\}/\{3 - \mu\,\mathrm{Cot}\,\theta\}] \quad (1)$$

where θ is the semi-apex angle of the indenter and μ is the Coulomb friction coefficient. As a typical example, if the f values of Ce-TZP2 from Fig. 1(b) are considered, with $2\theta = 136°$, the μ values are estimated using eqn (1) as 0·19, 0·17, 0·21 and 0·17, corresponding to the normal loads of 8 N, 10 N, 13 N and 18 N, respectively. This implies a load-independent average Coulomb friction coefficient of $0{\cdot}19 \pm (0{\cdot}02)$. Thus, it appears that ploughing was the major component of deformation in the present materials.

The increase in scratch width and depth and hence in wear volume, see Figs 1(c), (d) and (e), with higher normal load is possibly a consequence of increased

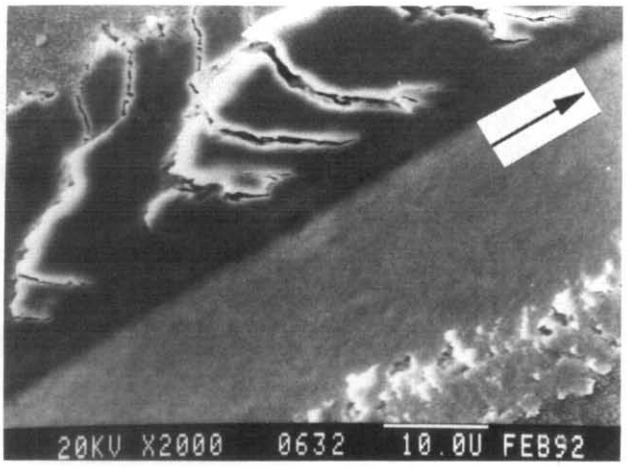

(a)

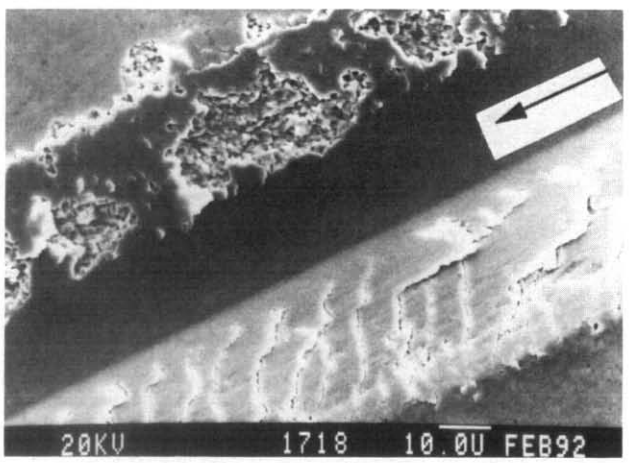

(b)

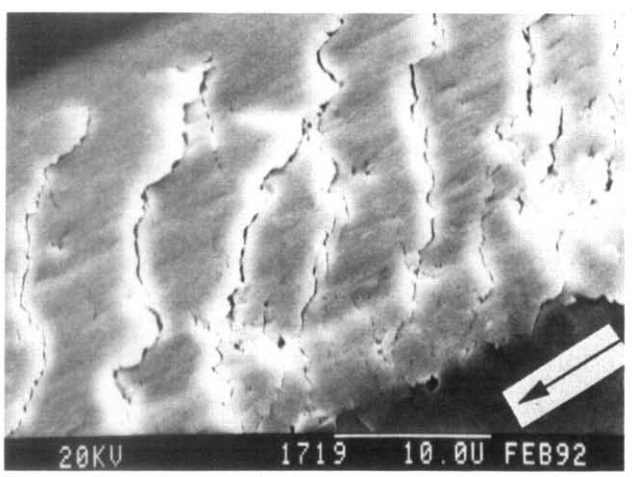

(c)

Fig. 6. (a) Microcracking and grain boundary microfracture in the scratch made at 13 N load on 0·5 μm grain size Ce-TZP; (b) microcracking and chipping in the scratch made at 18 N load on 1·0 μm grain size Ce-TZP; (c) details of the microcrack interaction shown in Fig. 6(b).

plastic deformation. Notice that there is no appreciable variation in these parameters with respect to changes in the grain size.

As indicated in Fig. 1(f), in sharp contrast to the behaviour of present Ce-TZP ceramics, there exists a strong influence of grain size in wear behaviour of alumina ceramics. This has been shown[14] to be qualitatively explainable in terms of a crack mechanics based model. Briefly, the existence of high residual stress in alumina ceramics was found to exert a significant influence on relative ease or difficulty of grain boundary microcracking. Based on SEM observations of frequent grain boundary microcracks originating from triple grain junction pores in the wear groove of coarse-grained aluminas, the relative ease or difficulty of grain boundary microcracking was shown to be linked to the amount of contact damage stress necessary to initiate microcracking. It was found that the amount of contact damage stress required to initiate grain boundary microcracking was much larger in the 0·7 μm grain sized alumina in comparison to that of the 25 μm grain sized alumina. Consequently, the wear volume of fine-grained alumina was much lower than that of the coarse-grained alumina.

Coming back to the case of the present Ce-TZP ceramics, assuming that the two side planes adjacent to the leading plane are also in contact, the effective load bearing area of the groove amounts to 3/4 B^2, where B is the width of the groove. Then, the mean contact pressure, σ_c, is given by $P/(3/4\ B^2)$. Based on the experimental data of groove width, Fig. 1(c), the estimate of σ_c ranges from about 2 to 6 GPa. Interestingly, the data from Ref. 12 gives an estimate of 0·25 GPa for yield stress. This estimate compares favourably with the tensile yield stress data of 0·35 GPa measured for 12 mol% CeO_2-stabilised TZP ceramics.[18] Thus, it seems logical to assume that in the present experiments the nominal contact stress was greater than the flow stress. Such a situation would promote plastic deformation in the scratch groove, observed in Figs 5(a) and (b).

However, in the presence of a tangential frictional force, the exact contact stresses are likely to be much more complicated than what has been simplistically assumed here. For instance, the presence of frictional force in addition to the normal load would significantly enhance the tensile stresses at the trailing edge of the indenter.[19] In addition, the presence of friction at the interface between the ceramic and the sharp indenter would almost invariably lower the value of critical stress necessary to initiate grain boundary microfracture.[19,20] This aspect will be discussed later in further detail.

The increase in transformation zone widths with grain size and applied normal load, Figs 2 and 3, should be viewed in terms of autocatalysis of the stress-induced t → m transformation.[12,18] The current understanding of the t → m transformation supports a picture in which the transformation is nucleation controlled. It has been appreciated that the autocatalysis may be initiated by a multiple nucleation event.[18]

The probability of such nucleation would depend

on the availability of a nucleating defect. This probability, in turn, is a sensitive function of the thermodynamic potential that acts as a driving force in terms of either temperature or stress. Now, it may be assumed that under similar conditions of applied normal plus tangential loading, the number of such thermodynamically potent defects which could nucleate t→m transformation would be much smaller in a fine-grained matrix than in a coarse-grained matrix. In other words, the autocatalytic effect may be expected to be activated much more easily in a coarse-grained matrix than in a fine-grained one.[18] This means that the number of transformable grains may be relatively smaller in a fine-grained matrix than in a coarse-grained matrix of Ce-TZP. Consequently, the transformation zone would be rather narrow in the fine-grained matrix, as observed in Figs 3(a) and (b) for 0·5 μm grain sized Ce-TZP. Using similar logic, the relatively larger transformation zone size in the Ce-TZP material of the largest grain size, e.g. 2·7 μm, may be anticipated, see Figs 3(c) and (d).

Also, it is interesting to note that the width of the transformation zone changes much more rapidly in going from 0·5 μm to 1·0 μm grain size than in going from 1·0 μm to 2·7 μm grain size, at any given applied load, e.g. 8 N or 18 N, during the single pass scratch experiments; see Fig. 2. This implies that possibly the grain size of 1·0 μm is critical in terms of stress-induced transformation in the present Ce-TZP ceramics. Since the stress-induced t→m transformation also leads to irreversible processes such as dislocation generation, microcracking and twinning,[6,10,11,18] which, again is a grain size dependent process, the existence of a critical grain size may be expected. Indeed, a sharp transition is reported to occur at a grain size of 1·0 μm in the transformation zone size on the tensile surface of the present materials in the course of *R*-curve experiments.[12] However, in those experiments, the transformation zone size, h, increased to a maximum with increase in grain size from 0·5 μm to 1·0 μm but decreased thereafter with further increase in grain size to 2·7 μm. Comparison of the results of the present work, Fig. 2, with those in Ref. 12, seem to imply that depending on loading configurations there can be significant variations in the extent of t→m transformation and hence, in the grain size dependence of the transformation zone size in Ce-TZP materials.

At a given grain size, the load dependence of the measured transformation zone size, Fig. 2, may be a consequence of the stress-induced t→m transformation process itself. It has been noted[18] that once the autocatalysis process is initiated, multiple nucleation events may follow in a stimulated fashion to enable further transformation to propagate quickly over an extended region. At higher applied loads, better stress assistance being externally provided, the nucleation probability is also effectively enhanced. If this were the scenario, one would expect a higher amount of t→m transformation to be involved in the relatively coarse-grained materials compared to the fine-grained material, given the similar amount of enhancement in externally applied stress system. A more detailed examination of Fig. 2 indicates that increasing the applied load in the single pass scratch experiments from 8 N to 18 N enhances the transformation zone size by about 10 μm only in the Ce-TZP1 material of 0·5 μm grain size, whereas in the relatively coarse-grained materials the zone size enhancement is by about 20–30 μm.

It has been already mentioned that based on measured data of groove width the nominal contact stresses in the present experiments were in the range of 2 to 6 GPa, whereas the stress required to induce t→m transformation is reported to be 0·23 to 0·29 GPa.[12] Now, the presence of tensile stress can trigger t→m transformation, provided the requisite magnitude is attained.[4,10–12] In view of the pressure-hardening effect associated with the transformation plasticity in Ce-TZP materials,[6] it would seem reasonable to assume that the scratching process with the sharp indenter is causing an elastic–plastic stress field rather than a purely elastic or a purely plastic one. Analytical solutions assuming pure elastic deformations for a sharp indenter under normal plus frictional force[19] is, hence, not applicable.

However, the stress field beneath a moving sharp indenter in a purely elastic solid is found to be similar to that of a quasi-static indentation except for the fact that in the moving case the stress field is slightly asymmetrical. Unfortunately, a complete analytical solution of a sharp pointed indenter moving under normal plus tangential force in an elastic-plastic solid is not available either. However, following Ref. 19, it may be assumed that the actual stress field beneath the moving indenter is somewhat closer to that under elastic–plastic indentation in a pressure-hardening solid.[6]

The plastic zone about a hardness impression can be assumed to be similar to that in front of a moving indenter. This situation can be idealised to the expansion of the front half of a spherical cavity under internal pressure.[6,19] In terms of spherical polar coordinates, the stress σ required to produce plastic flow to a radius b surrounding a half-spherical hole of radius a in a solid with pressure-hardening coefficient α and yield stress Y_0 is given by[6]

$$\sigma = (Y_0/\alpha[(b/a)^{2\alpha/1+\alpha}] + (2Y_0/3 + \alpha)(b/a)^{2\alpha/1+\alpha} \quad (2)$$

The radius a is related to the diagonal $2a_1$ of the Vickers indentation by $a = 0{\cdot}45\, a_1$.[6] Now, assuming

$a_1 = B/2$ where B is the measured value of groove width

$$b = (B/2) + h$$

where h is the transformation zone width beside the scratch, gives $b/a \cong 6$ for the scratch made at 8 N load in the Ce-TZP1 material. The value of E/H, where E is the Young's modulus and H is the hardness, is found to be $\cong 25$ from Ref. 12. The corresponding value of the pressure-hardening coefficient $\alpha \cong 1$ on extrapolation from Fig. 3 of Ref. 6. Using the measured b/a value with this value of α in the eqn (2) estimates α to be $\cong 8\,Y_0$. This is of course a very crude estimate. However, since it has been demonstrated[19] that the presence of a tangential force always enhance the tensile stress magnitude over and above that developed due to the static contact event because of the presence of strong interfacial friction, it seems reasonable to assume that the actual stress field should have a magnitude of $\geq \sigma$.

For the present Ce-TZP ceramics Y_0 is $\cong 0{\cdot}25$ GPa.[12] Then, the stress field required to produce the observed deformation zone size is about 2 GPa. If it is assumed that the tensile component of the stress field that occurs behind a moving sharp indenter[19] supplies this stress, then a very rough estimate of the tensile stresses involved should be $\cong 2$ GPa which is significantly higher than that required, e.g. 0·23 GPa to 0·29 GPa,[12] to initiate stress-induced t→m transformation in the present Ce-TZP materials.

4.2 Wear mechanisms

As indicated in Section 4.1, the main deformation mechanism was ploughing by the pyramidal indenter through the material. The micrographs presented in Figs 5 and 6 seem to support this contention. However, ploughing was not the sole component of deformation. Some very localised microcracking, particularly near the edges of the groove, always occurred. Large-scale brittle fracture-induced material removal was essentially absent in these materials. These observations are in sharp contrast to the authors' observations in the case of sintered alumina of grain size $>0{\cdot}7\,\mu$m where a brittle fracture-controlled wear mechanism dominated in similar scratch tests as reported here.[14]

Several factors may be responsible for the observed microcracking, see e.g. Figs 5(c) and (d). It is highly probable that the two adjacent faces to the leading plane were in contact with the deformed material. The high interfacial friction between those side planes and the deforming material may cause significant localised stress particularly near the sharp corners of the pyramidal indenter, if the leading plane is slightly rotated during the scratching process. If such stresses are of sufficient magnitude they may cause asymmetric deformation and localised microcracking, as observed in Figs 5 and 6. The other factor responsible may be mechanically or thermally induced t→m phase transformations.[2,6,10,11] The thickness of the transformation layer may be less than the grain size in PSZ but may involve a few grain dimensions in Y-TZP and Ce-TZP ceramics.[2,4,11,21]

It has been indicated above that tensile stress should be approximately ≥ 2 GPa. The stress required for t→m transformation being much smaller, e.g. 0·23 to 0·29 GPa, the transformability criterion is amply satisfied. Consequently, a thin surface layer in the groove is heavily deformed, which results in the realisation of the t→m transformation. Figure 5(d) indeed indicates a heavily deformed sub-surface layer lying close to the groove. The associated volume expansion of about 3–5% is unlikely to be accomodated in the otherwise continuous microstructure.[1,2,18] As the deformed, phase-transformed layer of material tries to push its way through the surrounding bulk material, internal stresses may be developed in the grain boundaries. Eventually, the generation of microcracks in the grain boundaries would help the process of relieving this excess internal stress.

Depending on the orientation of a particular grain or grain assembly with respect to the surrounding microstructure, the ease of microcracking and intergranular fracture should be ultimately decided. Figure 5(c) illustrates the presence of both grain boundary microcracking as well as intergranular crack propagation in the near-surface region of 0·5 μm grain sized material. The angle of these cracks vary between 30° and 60° with respect to the sliding direction, see Figs 5(c) and 6(a) and (c). It is suggested that these cracks may originate due to the combined action of the high tensile stress field present in the wake of the indenter plus the shear stress.[19,22]

Plane strain cracks in glass are reported to grow at an angle to the crack plane when subjected simultaneously to both mode I and mode II loading.[29] While the mode I loading corresponds to the normal stress application situation, the mode II loading corresponds to shear loading of the crack. It has been appreciated that the shear stress distribution beneath the contact is quite significant in the case of a sharp indenter subjected simultaneously to both normal and tangential loading with respect to the counterface material.[19] Thus, the presence of these microcracks should be viewed not only in terms of the normal stress but also in terms of the shear stress distribution in the Ce-TZP material. The sense of the angle, in most of the present cases, is consistent with that predicted by the mixed-mode crack growth theory.[23] However, the net shear stress

present in the contact shall also be influenced by the stress pattern actually involved in the observed $t \rightarrow m$ transformation process.

In view of the complexity of the transformation process itself,[6] an exact estimation of the shear stresses involved in dry sliding of a sharp indenter on a phase-transforming ceramic such as Ce-TZP is, unfortunately, yet to be available. In absence of the exact stress estimation, a comparison of the observed crack growth angles with the crack growth angles as predicted by the theory of mixed-mode loading,[23] is inhibited. However, it is interesting to note that similar cracks are observed in polycrystalline ceramics as well as in glass subjected to sliding sharp contacts.[24,25] As a matter of fact, even a blunt contact like that of a steel ball is reported to induce a parallel array of partial cone cracks in glass during dry sliding experiments.[26]

Nevertheless, these microcracks often seem to get blunted in the course of their extension through the microstructure, see Fig. 5(c). It is suggested that as the microcrack grows the crack front gets further away from the location of highest stress concentration. As a result, the effective stress intensity on the crack front is reduced. In the process the microcrack gets arrested. It may be noted additionally from the microdamage patterns observed, e.g. Figs 5(c), 6(a) and 6(c), that wherever they are present the cracks form a parallel bunch. It is suggested that the presence of such a parallel bunch of microcracks may be linked to the statistical distribution of asperities[26] on the sliding sharp indenter.

Increasing the normally applied load usually resulted in small amounts of localised grain boundary microfracture, Fig. 6(a), and to a limited extent localised chipping and microcrack interaction, Fig. 6(b) and (c). Possibly the microcracks are generated at regions of steepest stress gradient in the microstructure. It is suggested that the case of microcrack generation may be similar to what would be seen in metals due to the exhaustion of work-hardening in the highly strained regions. However, here it may be related to the exhaustion of the transformation toughening effect.[1,6,11,18] Eventually, as these microcracks join together on the surface and below it, a thin layer of material may be detached, giving rise to the appearance of localised chipping in the groove, Fig. 6(c). Further examination by transmission electron microscopy of the scratches is, however, necessary to give better validity to the suggestions presented here.

Thus, phase-transforming ceramics such as the present Ce-TZP ceramics exhibit a wear mechanism with predominance of the ploughing component. Further, the wear volume exhibits no significant dependence on grain size. This is in sharp contrast to the previous observation of strong grain size effect in abrasive wear of alumina.[14] There, the wear mechanism exhibited brittle fracture control at grain size higher than 0·7 μm. It has already been briefly indicated that in the alumina ceramics the residual stresses played a significant role in determining the wear behaviour. Similar factors may not be of vital significance for the present Ce-TZP ceramics, at least in terms of their wear behaviour.

So, the beneficial effect of grain coarsening, e.g. the Ce-TZP1 material of grain size 0·5 μm having a steady-state toughness of 10·7 MPa$\sqrt{\text{m}}$ in comparison to the Ce-TZP2 material of grain size 1·0 μm having a steady-state toughness of 16·7 MPa$\sqrt{\text{m}}$, may be utilisable without sacrificing much in terms of wear resistance. The same may not be true of other TZP ceramics.

For example, Y-TZP ceramic containing 2 mol% Y_2O_3 and having a steady-state toughness of 9·2 MPa$\sqrt{\text{m}}$ suffers significantly large wear loss through grain fracture, while another Y-TZP ceramic with 3 mol% Y_2O_3 and having a steady-state toughness of 5·2 MPa$\sqrt{\text{m}}$ suffers only mild wear damage when exposed to similar experimental conditions.[4] In other words, highly transformable ceramics suffered large wear loss in these experiments. Thus, even in the case of TZP ceramics, whether the beneficial effect of grain coarsening and/or transformation toughening resulting in a rising crack growth resistance characteristics can be utilised without sacrificing the wear resistance depends on the particular application sought for. Possibly one would need to look for an optimised microstructure incorporating the idea of higher steady-state toughness and a reasonable wear resistance.

In the case of a non-phase-transforming ceramic such as alumina, to achieve such a situation appears even more challenging. The reason seems to lie in the strong grain size effect on abrasive wear of alumina, as demonstrated by several workers.[14,16] In the case of alumina, the recent findings are that the more toughened the material is the larger is the abrasive wear damage when the toughening occurs predominantly through crack bridging in a coarsened microstructure.[16] Clues to this effect have recently been elaborated in the present authors' work on alumina[14] where it has been demonstrated to be linked to the presence of residual stresses in the microstructure. In other words, also in the case of non-phase transforming ceramics it may be necesary to optimise the microstructure for wear resistant applications. Of course, here the design problem could be even more subtle than in the case of phase-transforming ceramics.

Finally, the design of microstructure should be finally decided by the ultimate application for which the material is developed. It is imperative that one

may need to make a trade-off between the toughening parameters and the wear resistance depending on the particular commercial need which will also govern the choice of a particular class of ceramic.

5 Conclusions

Single pass scratch experiments were conducted with a Vickers pyramid moving at a constant speed of 6 mm/s under normal applied loads of 8 N to 18 N on 9 mol% Ce-TZP materials with grain sizes of 0·5 μm, 1·0 μm, 1·4 μm, 1·5 μm and 2·7 μm. The results of these experiments were additionally compared with the authors' previous work on alumina ceramics[14] to highlight the distinction in the behaviour of alumina and zirconia ceramics under dry sliding situation at high contact stress level. From these investigations the following conclusions are drawn:

(a) In the case of a typical phase-transforming ceramic, e.g. the present Ce-TZP ceramics, for a given grain size the width (B), depth (D), and hence, wear volume of the scratch groove and the width of the transformation zone (h) surrounding the scratch increased with the normal load. There was no significant influence of the grain size on width depth or volume of the wear groove. However, at a given load, the width of the transformation zone increased with the increase in grain size. Particularly in the coarse-grained materials, the transformation zone was characterised by considerable surface uplift indicating significant influence of transformation plasticity in the process. These observations could be rationalised in terms of the stress-induced t $\rightarrow$ m transformation and the autocatalytic nature of the phase transformation.

(b) Plastic ploughing and very small amount of microcracking, grain boundary microfracture and chipping characterised the wear mechanism of the present Ce-TZP ceramics. These observations are suggested to be a consequence of the stress-induced transformation in the contact zone. The alumina ceramics, on the other hand, exhibited a strong grain size effect in their abrasive wear behaviour.[14] This is in sharp contrast to the behaviour of Ce-TZP ceramics investigated here. The basic wear mechanism in alumina ceramics of grain size higher than 0·7 μm involved brittle fracture control, while the fine-grained alumina of grain size 0·7 μm exhibited a mixed control of plastic deformation and brittle fracture. This evidence suggests that there exist considerable differences in the deformation and wear behaviour of a phase-transforming ceramic such as the present Ce-TZP ceramics and a typical non-phase-transforming ceramic, e.g. alumina, when exposed to similar dry sliding contact at significantly high stress levels.

Acknowledgements

Y.-W. Mai wishes to thank the Australian Research Council (ARC) for the continuing support of this project and A. K. Mukhopadhyay (AKM) acknowledges the award of an ARC Post-doctoral Fellowship tenable at the University of Sydney and a study leave from the Central Glass & Ceramic Research Institute, Calcutta 700032, India. The keen interest of the Director, Central Glass & Ceramic Research Institute, in the present work is also sincerely appreciated. The Sydney University Electron Microscope Unit and CSIRO, Division of Applied Physics at Sydney, have kindly provided access to their facilities. AKM wishes to thank F. Wilshaw and E. G. Thwaite for experimental assistance and valuable discussions.

References

1. Green, D. J., Hannik, R. H. J. & Swain, M. V., *Transformation Toughening of Ceramics*. CRC Press Inc., Florida, USA, 1989.
2. Bundschuh, W. & Zum Gahr, K-H., Influence of porosity on friction and sliding wear of tetragonal zirconia polycrystals. *Wear*, **151** (1981) 175–91.
3. van Groneou, A. B., Maan, N. & Veldkamp, J. D. B., Scratching experiments in various ceramic materials. *Phillips Research Report*, **30** (1975) 320–59.
4. Birkby, I., Harrison, P. & Stevens, R., The effect of surface transformation on the wear behaviour of zirconia TZP ceramics. *J. Eur. Ceram. Soc.*, **5** (1989) 37–45.
5. Chen, I.-W., Implications in transformation plasticity in ZrO_2-containing ceramics: II, elastic–plastic indentations. *J. Am. Ceram. Soc.*, **69** (1986) 186–94.
6. Hannik, R. H. J., Murray, M. J. & Scott, H. G., Friction and wear of partially stabilised zirconia: basic science and practical application. *Wear*, **100** (1984) 355–66.
7. Stachowiak, G. W. & Stachowiak, G. B., Unlubricated friction and wear behaviour of toughened zirconia ceramics. *Wear*, **132** (1989) 151–71.
8. Trabelsi, R., Treheux, D., Orange, G., Fantozzi, G., Homerin, P. & Thevenot, F., Relationship between mechanical properties and wear resistance of alumina–zirconia composite. *Tribol. Trans.*, **32** (1989) 77–84.
9. Fischer, T. E., Anderson, M. P., Jahanmir, S. & Salher, R., Friction and wear of tough and brittle zirconia in nitrogen, air, water, hexadecane and hedecane containing stearic acid. *Wear*, **124** (1988) 133–48.
10. Swain, M. V. & Hannik, R. H. J., Metastability of the martensitic transformation in a 12 mol% ceria–zirconia alloy. *J. Am. Ceram. Soc.*, **72** (1989) 1358–64.
11. Hannik, R. H. J. & Swain, M. V., Metastability of the martensitic transformation in a 12 mol% ceria–zirconia

alloy: I, deformation and fracture observations. *J. Am. Ceram. Soc.*, **72** (1989) 90–8.
12. Grathwohl, G. & Liu, T., Crack resistance and fatigue of transforming ceramics: II, CeO_2-stabilised tetragonal ZrO_2. *J. Am. Ceram. Soc.*, **74** (1991) 3028–34.
13. Mukhopadhyay, A. K. & Mai, Y.-W., Deformation characteristics in scratching of fine grained alumina ceramic. *J. Mater. Sci.*
14. Mukhopadhyay, A. K. & Mai, Y.-W., Grain size effect on abrasive wear mechanisms in alumina ceramics. *Wear*, **162–164** (1993) 258–68.
15. Moore, M. A. & King, F. S., Abrasive wear of brittle solids. *Wear*, **60** (1980) 123–40.
16. Cho, S. J., Hockey, B. J., Lawn, B. R. & Bennison, S. J., Grain size and *R*-curve effects in abrasive wear of alumina. *J. Am. Ceram. Soc.*, **72** (1989) 1249–52.
17. Goddard, J. & Wilman, H., A theory for friction and wear during abrasion of metals. *Wear*, **5** (1962) 114–35.
18. Reyes-Morel, P. E. & Chen, I.-W., Transformation plasticity of CeO_2-stabilised tetragonal zirconia polycrystals: I, stress assistance and autocatalysis. *J. Am. Ceram. Soc.*, **71** (1988) 343–53.
19. Swain, M. V., Microfracture about scratches in brittle solids. *Proc. Royal Soc. London*, **A366** (1979) 575–97.
20. Evans, A. G. & Wilshaw, T. R., Quasi-static solid particle damage in brittle solids—I, observations, analysis and implications. *Acta Metall.*, **24** (1976) 939–56.
21. Hwand, B., Houska, C. R., Ice, G. E. & Habenschuss, A., X-Ray analysis of near surface phase distribution of the wear of a PSZ disc. *Adv. Ceram. Mater.*, **3** (1988) 180–3.
22. Kimura, Y. & Shima, M., Stress intensity at surface cracks in sliding wear: a parametric study. In *Proceedings of the Japan International Tribology Conference*, Nagoya, Japan, 1990, pp. 569–74.
23. Erdogan, F. & Sih, G. C., On the crack extension in planes under plane loading and transverse shear. *Trans. ASME. Ser. D, J. Basic Eng.*, **85** (1963) 519–27.
24. Chen, S. Y., Farris, T. N. & Chandrasekar, S., Sliding microindentation fracture of brittle materials. *Tribol. Trans.*, **34** (1991) 161–8.
25. Veldkamp, J. D. B., Hattu, N. & Snijders, V. A. C., Crack formation during scratching of brittle solids. In *Fracture Mechanics of Ceramics*. Vol. 3, ed. R. C. Bradt, F. F. Lange, A. G. Evans & D. P. H. Hasselmaan. Plenum Press, NY, USA, 1976, pp. 273–301.
26. Lawn, B. R., Wiederhorn, S. M. & Roberts, D. E., Effect of sliding friction forces on the strength of brittle materials. *J. Mater. Sci.*, **19** (1984) 2561–9.